The stabilizing effect of geoengineering on the Atlantic Meridional Overturning Circulation

Niek Collot d'Escury

July 19, 2019

Abstract

Solar radiation management has been proposed to enhance earth's albedo and reduce the amount solar radiation retained by the earth. Here we analyse the effects of the strategic injection of sulphate aerosols into the stratosphere on one of the ocean 's large scale circulations. The aerosols are injected at four strategic locations (30°, 15° in both hemispheres) to minimize the future change in the global mean temperature and the temperature gradients between hemispheres and from equator-to-pole. The approach is successful at keeping the temperature goals at the predefined 2020 levels of the RCP 8.5 scenario. This means some adverse effects of solar radiation management, like the 'over cooling of the equatorial region are reduced compared to previous studies. However, feedbacks from surface fluxes cause a strengthening of the Atlantic Meridional Overturning Circulation (AMOC) under the injection of sulphate aerosols compared to a warming climate under a RCP 8.5 scenario. How and what exactly causes this difference in strength and stability of the AMOC is critical for our understanding of the complete response of the climate. The understanding of the shifts in the strength and stability of the AMOC is important because of the role the AMOC played in some of the largest shifts in the global Paleoclimate. Studying the simulations of the geoengineering large ensemble project gives us new insights in the strength and stability of the ocean's circulation, but also highlights the fact that we need more research in the climate's response to geoengineering strategies before implementation is a viable option to reduce the global temperature.

1 Introduction

Despite the implementation of many mitigation strategies agreed on in the Paris agreement (2015), the global temperature continues to rise. In theory, mitigation is capable of reducing the greenhouse gas emissions to the required levels in order to keep the temperature rise below 2 degrees. To accomplish this mitigation goal countries have submitted Intended Nationally Determined Contributions (INDCs), which outline their post 2020 climate goals. Rogelj (2016) shows that these INDCs are not enough to keep the temperature rise below 2 degrees (see fig. 1)[1]. Because of this, alternative approaches have received more attention, like geoengineering methods. Geoengineering methods are meant to offset anthropogenic emissions by either removing CO_2 from the atmosphere (negative emissions) or by increasing earth's albedo (solar radiation management) [2][3].

Keller (2015) compared different negative emission methods with solar radiation management (SRM), and found that out of these methods SRM had the largest potential [3]. Out of the different SRM methods currently being researched the injection of sulphate aerosols into the stratosphere is the most feasible in the near future. This method creates a reflective veil by injection sulphur gases, like SO_2 into the stratosphere. The injected SO_2 reacts with hydroxide (OH) to form the reflective sulphate aerosols (H_2SO_4). The injection must be at high altitudes (stratosphere) because lower in the troposphere the aerosols will rain out before they can achieve their optimal potential for cooling. The principle of injecting sulphate aerosols in the stratosphere is a method derived from the eruptions of large volcanoes. Volcanic eruptions, like the Pinatubo eruption of 1991, have proven that sulphate aerosols have a quick and significant cooling effect [4]. Cost-benefit analysis even showed that the costs of climate damages or large scale mitigation are much higher compared to the use of SRM [5].

Modelling studies have assessed the effectiveness of SRM, which showed that SRM is probably capable of offsetting the predicted global warming. But the precise effects of SRM on all the individual components of the climate system is still under investigation. Robock (2008) lists some of the negative consequences the use of SRM can have on the climate and the world in general [6]. To get a better understanding of the effects of the injection of sulphate aerosols (from here on referred to as geoengineering) on the climate we focus in this paper on the impact on the Atlantic Meridional Overturning Circulation.

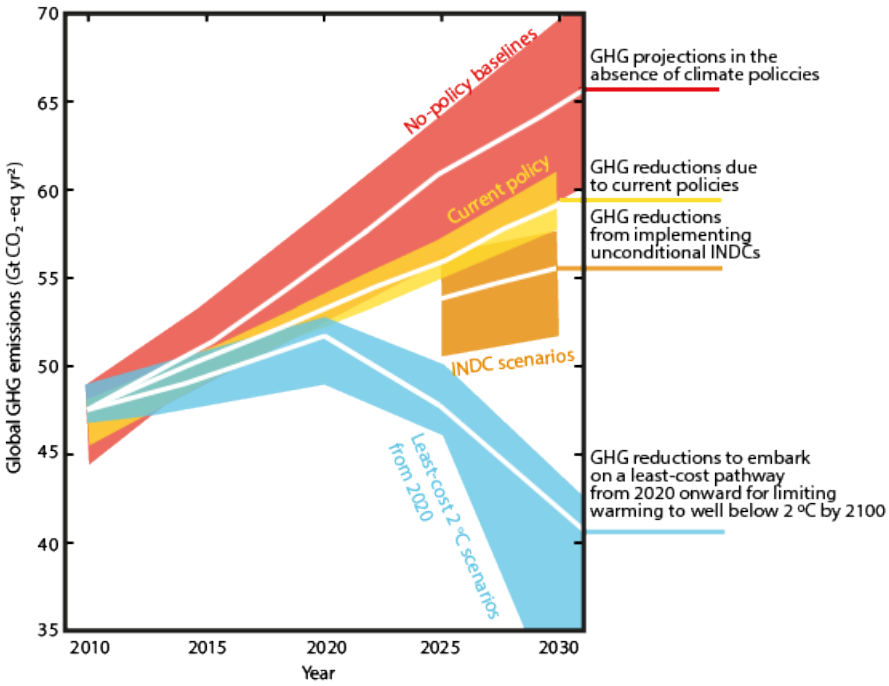

Figure 1: Global green house gas emissions comparison between scenarios with no-policy, current policy, INDCs and 2 ^{o}C degree. The white lines indicate median of the ranges. The no-policy and 2 degree scenarios show the 20th-80th percentile while the current policy and INDCs show the 10th-90th percentile [1].

Current knowledge of the Atlantic Meridional Overturning Circulation

The large-scale ocean circulation is a vital component of the climate system and one of the major components of this circulation is the Meridional Overturning Circulation (MOC). In this paper we are interested in the branch of MOC, which is located in the Atlantic basin and is referred to as the Atlantic Meridional Overturning Circulation (AMOC). Figure 2 shows a schematic zonally averaged cross section of the Atlantic basin. The wind driven upwelling and mixing driven upwelling are the main driving processes of the AMOC and can be found in the figure as the black and the wavy lines respectively. The wind driven upwelling is caused by the strong westerly winds over the Southern ocean that induce a northward water transport at right angle to the wind, Ekman transport. The Ekman transport is a divergent water flow causing upwelling of deep water in this region. The mixing driven upwelling is caused by mixing along the density gradient (diapycnal mixing) and by internal waves along the margin of the basin. Here we are interested in the formation of deep water in the Northern Atlantic, where buoyancy of surface waters is influenced by changes in surface fluxes of freshwater and heat [7].

The AMOC has been weakening significantly since 1880 due to changes in surface fluxes. By comparing a high resolution climate model with measured data from the *rapid climate change* (RAPID) transatlantic mooring array, Ceasar et al. found a Sea Surface Temperature (SST) fingerprint explaining changes in the AMOC strength. The fingerprint consists of a cooling in the sub-polar Atlantic and a warming and northward shift of the Gulf stream associated with a weakening of the AMOC strength. With the help of the fingerprint Ceasar et al. were able to construct an evolution of the AMOC strength since 1880 [8]. This showed that the AMOC strength is presently at a record all time low.

There are large uncertainties in future predictions of the AMOC, but it is a certainty that continued global warming will further weaken the AMOC [9][7]. A continued weakening of the AMOC under climate change could cause the AMOC to shift to an 'off' state. Stommel (1961) was the first to suggest the existence of two AMOC states, either 'on' or 'off'. The importance of a shift between these states has been found by linking shifts in the global climate (from warm to cold, Dansgard-Oescher events) during the last glacial maximum with shifts in the AMOC [10] [11] [12]. The bistabillity is cause of much debate, since the current climate models have trouble predicting whether the AMOC is a mono or bistable state (see section 2.3).

The ocean-atmosphere interaction goes both ways. So a change in the climate will also impact the AMOC. As mentioned above changes to the surface fluxes change the buoyancy and thus the sinking speed of the AMOC (as can be seen in Fasullo, 2018 [13]). Two feedback mechanisms governing multiple equilibrium states of the

AMOC give more insight in the effect of changing surface fluxes on the physical mechanisms of the AMOC. The advective feedback is a feedback on the meridional density gradient, which is a driving force of the circulation. The current state of the AMOC ('on') is thermally driven where the heating of the lower latitudes and the cooling of the higher latitudes by the surface heat flux has a stronger effect than the salting of the lower latitudes and freshening of the higher latitudes by the freshwater flux. If a perturbation in AMOC strength increases the salt transport to the north the sinking is enhanced, but the increased strength also transports more heat north lowering the sinking speed again. This heat transport is therefore a negative feedback on the AMOC strength. Due to differences in the response time of salinity and temperature anomalies, a negative feedback can be caused by a freshwater perturbation in the Northern Atlantic. The weakening of the density gradient causes reduced transport of heat and salt northward lowering the sinking speed. The heat anomaly is quickly damped by an atmosphere response but the freshwater anomaly is not damped and causes a positive feedback on the AMOC strength [14].

The second feedback mechanism, is a convective feedback where mixing between surface and deep water occurs if the surface waters are denser than the deep water. In a convective state fresh/cool waters are mixed down while warm/salty water is mixed to the surface. Here the heat lost to the atmosphere creates denser waters again and maintains the convection [14].

As mentioned above, a shift in the state of the AMOC can have large and far-reaching consequences around the world. Some of these consequences are sea level rise, temperature change and a shift in the position of the Inter Tropical Convergence Zone (ITCZ). The effect of the sea level is a complicated and dynamical effect, but the result for the countries surrounding the Northern Atlantic basin will be significant sea level rise. This is caused by the lack of sinking of cold waters in the Northern Atlantic, which warms and thus expands the deep water. The effect on the temperature is also largely limited to the countries surrounding the Northern Atlantic basin. Here the temperature will lower because of the lack of warm surface waters flowing from the south[8][15]. A more global impact will be the change in the position of the ITCZ. Without heat transport by the ocean, the position of the ITCZ would be determined purely by the radiative forcing from the sun. This would result in a mean position at the equator. But because of the heat transported to the north by the AMOC, the position is shifted northward ($\pm 5\ ^{o}$C), which results in a heat transport to the south. An increase in heat transport by the AMOC results in a increase in strength of the ITCZ and shift further north [16].

In this paper we investigated whether geoengineering is capable of stabilizing the AMOC. This is done by analysing the data of two large ensemble simulations, one with geoengineering and one without (see section 2.1).

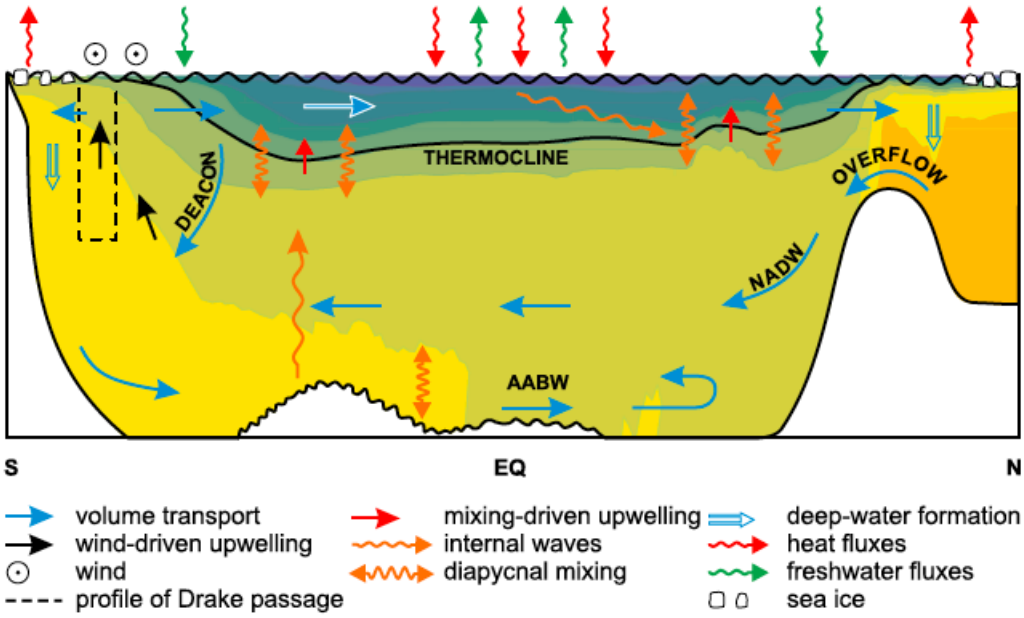

Figure 2: Schematic meridional cross section representing a zonally averaged view of the Atlantic basin. The straight arrows indicate the AMOC and the colour shading depicts the density profile derived from observational data. The thermocline is a region with a large temperature gradient and separates the light and warm upper waters from the denser and cooler deep waters. The two main upwelling mechanisms, wind driven and mixing driven, are displayed as the black lines and the wavy lines respectively. Wind driven upwelling is caused by a northward flow of the surface waters in the Southern Ocean (Ekman transport) due to strong westerly winds. Since the Ekman transport is a divergent flow, water wells up from depth. The mixing driven upwelling is caused by mixing along the density gradient (diapycnal mixing). This mixing is partly caused by internal waves along the ocean's margin. Deep water (Antarctic bottom waters, AABW; North Atlantic Deep Water, NADW) forms in the high northern and southern latitudes. The locations of deep water formation are tightly linked with the surface fluxes of heat and freshwater. These fluxes influence the sinking of the surface waters through their effect on the buoyancy. The Deacon cell in the Southern Ocean is a recirculation cell, which recirculates part of the wind driven transport [7].

2 Methods

In this section we will describe the model and give a detailed overview of the methods we used to analyse the changes in the AMOC. These methods are divided in the ocean-atmosphere response and a way to analyse the bistability of the AMOC using the salinity budget.

2.1 Model

We use simulations made available by the Geoengineering Large Ensemble project (GLENS)[17]. GLENS made use of the fully coupled Climate Earth System Model (CESM, version 1.5). The atmosphere was represented by the Whole Atmosphere Community Climate Model (WACCM). The Atmospheric chemistry of WACCM was updated with the Modal Aerosol Model (MAM3) to include the capability to inject SO_2 and the subsequent formation of sulphate aerosols, through oxidation with changing OH. MAM3 includes detailed aerosol processes including nucleation, coagulation, evaporation and sedimentation. More in depth descriptions of the CESM1(WACCM) and MAM3 models can be found in Hurell (2013) and Liu (2012) [18][19]. The ice component (CICE4) models only sea ice.

Model Setup
The GLENS project ran two simulations. One with only a transient CO_2 concentration and one with both a transient CO_2 concentrations and geoengineering. The CO_2 concentrations are prescribed by the Representative Concentration Pathway 8.5 (RCP 8.5). This pathway follows a high anthropogenic greenhouse gas emission scenario, which results in a 8.5 W/m^2 increase in radiative forcing [20].

In the simulation with geoengineering, it is attempted to keep certain large-scale features of the temperature field at their 2020 levels by means of SRM. A strategy to minimize changes in the global mean temperature (T0) and the global temperature gradients (between hemispheres, T1 and between equator and pole, T2) was devised by Kravitz (2017) [21]. The choice for these 3 degrees of freedom as opposed to one degree of freedom with a uniform distribution of aerosols, arises from uneven seasonal and latitudinal dependencies of insulation between the equator and poles. These dependencies result in an over cooled equator and under cooled poles, resulting in continued polar ice loss [22].

The strategy for keeping the three temperature targets (T0, T1 and T2) at the predefined 2020 levels resulted in four injection sites with different latitudes (30°N, 15°N, 30°S and 15°S) and identical arbitrarily chosen longitudes (180°E). The temperature targets were monitored and checked continuously and the injection rates adjusted when necessary. Because of the yearly increasing radiative forcing the aerosol concentration needs to keep increasing as well. Due to aerosol dynamics, like coagulation, the increase in aerosol concentration is not linear with the increase in radiative forcing. To increase the lifetime of the aerosols in the atmosphere the injection has to take place in the stratosphere, where the aerosols cannot be "rained out" (5 km above the tropopause) [23]. The 2020 level is defined an average of 2015-2025, which result in T0: 288.21 K, T1: 0.59 K and T2: -6.01 K.

Ensemble runs
The RCP 8.5 simulation is run with 21 ensemble members from 2010 to 2030. Three of these ensemble members continue to at least 2097 and one completes the run until 2099. The rest of the ensemble members do not make it to the end of the 21st century due to instabilities in simulating the RCP 8.5 scenario at the of the 21st century. We therefore only use the ensemble members that run till at least 2097. For each ensemble member initial conditions of the atmospheric state and the temperatures are slightly perturbed. The land, sea-ice and ocean state are identical for each ensemble member.

The geoengineering simulations are setup the same way as the RCP 8.5 simulation, but using the SO_2 injections to keep the temperature goals at the aforementioned 2020 levels. For the geoengineering simulation all members complete the run. All analyses are done with the mean of all 21 members. Further information about the GLENS project set-up can be found in Tilmes (2018) [17]

2.2 Ocean-atmosphere response

The strength of the AMOC is determined using the AMOC index (output field of the model), which is the zonally averaged stream function. We used the maximum strength over depth at 26N latitude, because this is the latitude where the RAPID measurements are being made.

To find the reason for a change in the AMOC we looked at the pattern of the Surface Heat Flux (SHF) and the sum of the precipitation, melt, run-off and evaporation (defined as negative). SHF is a sum of all heat fluxes at the surface: latent heat, sensible heat, shortwave radiation and longwave radiation. This flux is defined as

positive for a downward heat flux towards the surface. We defined the freshwater flux as PE with positive values for an increase in freshwater. For both fluxes we compared the average of the first 25 years with the pattern of the last 25 years. To compare the relative magnitude of both fluxes we converted them to a buoyancy flux with the following equation:

$$B = \underbrace{C_w^{-1} g\alpha Q}_{SHF} \underbrace{-g\beta S(E-P)}_{PE}$$

With C_w the specific heat capacity of sea water, α the thermal expansion of water, Q the surface heat flux, β the haline expansion and S the salt concentration [24].

We determined the response of the ITCZ due to a change in the AMOC strength by analysing the precipitation pattern in the Atlantic around the equator. We compared both the zonally averaged precipitation and the latitude of maximum precipitation calculated (eq. (1)). For both values we used a mask to look at the Atlantic (see fig 3a) and looked at the values between 20N and 20S.

$$\phi_{max} = \frac{1}{\lambda} \sum_{i=1}^{\lambda} \left[\frac{\int_{\phi_1}^{\phi_2} \phi \big(PA\big)^N d\phi}{\int_{\phi_1}^{\phi_2} \big(PA\big)^N d\phi} \right] \tag{1}$$

With ϕ the latitude, λ the longitude, P the PE, A the Area of each grid cell and N an exponent.

High exponents yield latitudes closer to the precipitation maximum. We used $N = 10$ based on research done by Adam (2016) that found that this exponent gives a reliable value for the maximum precipitation while smoothing some of the discretization noise [25].

2.3 Salinity budget

The salinity budget is part of the advective feedback mechanism of the ocean and is used here to evaluate the freshwater transport in the Atlantic basin. Rahmstorf (1996) formed a method for analysing the stability of the AMOC through the freshwater transport into the Atlantic basin at its southern boundary. This research formed the basis for the method used in papers by Dijkstra (2007) and Drijfhout (2011), which analyses the complete freshwater budget [26][11]. The complete freshwater budget (Evaporation minus precipitation and run-off and melt) can be written in short as:

$$\text{EPR} = Q_t + M + R_{es} \tag{2}$$

Equation (2) contains the change in time of the freshwater content, the advection of freshwater (M) and subscale transport (R_{es}). Q_t is a surface integral over the entire basin (see red area in fig. 3a) with positive values for an increase in the freshwater content. We do not calculate the subscale transport term here. The freshwater advection is calculated at the northern and southern boundaries of the basin (60N and 34S).

The modelled output is a curvilinear grid, which has curved latitudes in the north. This curvature complicates the choice for the northern boundary. We therefore chose a straight line, which lies close to the actual value of the 60N grid (see fig. 3b)

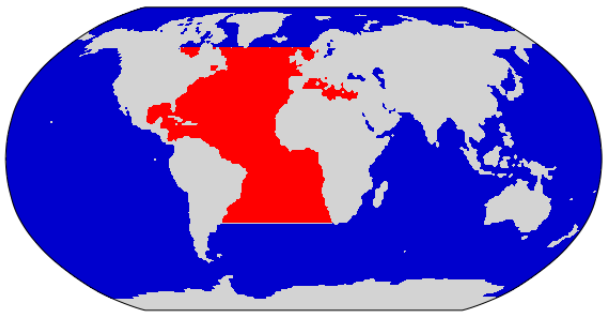

(a)

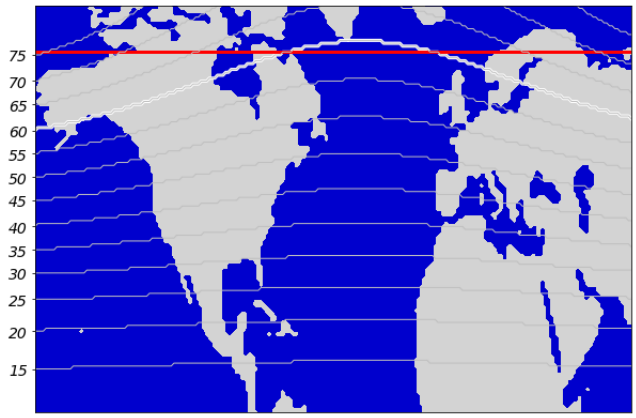

(b)

Figure 3: 3a is the Atlantic basin between 60N and 34S for a rectangular grid. 3b the curved grid lines are the modelled grid-lines of a curvilinear grid. The white line gives the 60N boundary and the red line indicates the boundary we used for the boundary in our calculation of the salinity budget.

The advection of freshwater can be divided in contributions from the azonal wind driven gyre transport (Maz) and in the zonal AMOC induced transport (Mov, eq. (3)). For both the Mov and Maz positive values mean transport of freshwater into the Atlantic basin [27].

$$Mov = -\frac{r_0}{S_0} \int_{\phi} (\langle v \rangle - \hat{v}) \langle S \rangle \cos\phi \mathrm{d}z \mathrm{d}\lambda \tag{3}$$

With S_0 the reference salinity, $(\langle v \rangle - \hat{v})$ the zonally-integrated baroclinic meridional velocity and $< S >$ the zonally averaged salinity.

The sign (direction of freshwater flow) of the Mov can be used as an indicator for the bistability of the AMOC. The bistability indicates whether the AMOC is capable of shifting between states. In a monstable state a perturbation will never be amplified and always be damped back to the original state.

A positive Mov is defined as a freshwater flow into the basin, which corresponds to a monostable AMOC state. The reasoning behind this, is that a weakening of the AMOC will transport less freshwater into the basin making the Atlantic saltier, which induces a negative feedback on the AMOC strength. For a negative Mov the reasoning is that with a weaker AMOC less freshwater is transported out of the Atlantic basin making the basin fresher and further weakening the AMOC (positive feedback on the AMOC strength) [28].

Many studies have been done on the verification of the theory of Rahmstorf (1996)[29]. However there is no consensus on the usefulness and validity of the stability criterion as defined by Rahmstorf. The theory of the Mov as a stability criterion assumes that the salinity of the Atlantic basin changes after a change in the AMOC driven transport. If other processes like gyre driven transport (Maz) or surface fluxes (PE) also change and balance the change in the Mov there is no reason to assume the stability of the AMOC is changed.

An improvement using a ΔMov has been suggested by Dijkstra (2007) and Lui and Lui (2013). Here they used:

$$\Sigma Mov = Mov_S - Mov_N$$

The ΣMov gives a better stability indicator because it looks at the convergence of freshwater, which gives more information about transport of freshwater into the Atlantic basin compared to transport through only the southern boundary. There is convergence and thus a stable regime if the transport from the south is positive and from the north negative [26][30].

The code we used to calculate all variables in the salinity budget is based on the work done by Toom (2014) and then adjusted to fit our ocean model [27].

3 Results

The AMOC in the geoengineering simulation (from here on referred to as geoengineering) strengthens between 2020 and 2060 (± 4 Sv). After this it remains relatively stable around 22 Sv (measure of ocean flow where 1 Sv = 10^6 cubic meters per second). This is in strong contrast with the RCP 8.5 simulation (from here on referred to as RCP) where after a relative stable period (2010-2030) we see a strong decrease in strength. The ±20% increase and ±35% decrease falls far outside of the typical inter annual variability of ±1 Sv [31].

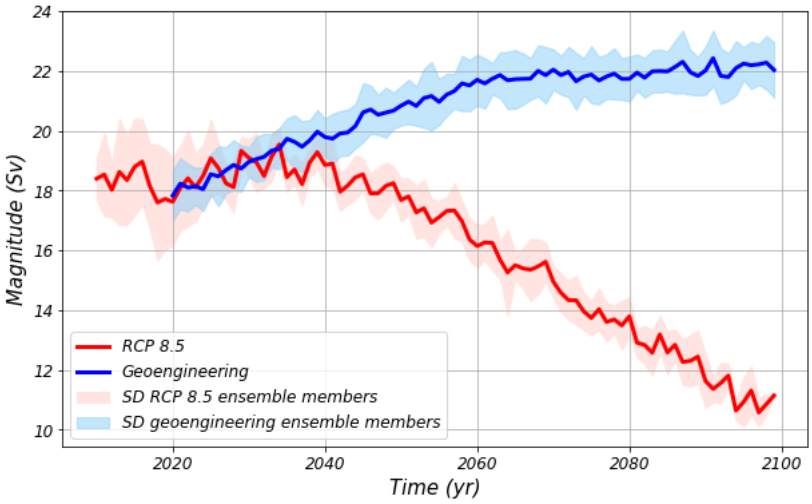

Figure 4: The maximum AMOC strength at 26.5^o N. The solid blue and red line are the yearly ensemble averaged geoengineering and RCP values respectively. The blue and red shaded fields are the standard deviations of all the ensemble members for both simulations.

3.1 Regional ocean-atmosphere response

As explained in the methods (see sec. 2.2) the differences in the surface flux patterns over time and between the two simulations can give detailed information about the cause of the change in the AMOC seen in figure 2. Figures 5a and 5b show the difference over time of the freshwater flux patterns for both the RCP and the geoengineering case. RCP is characterized by a intensification of the water cycle. The "wet" areas experience an increase in freshwater while the "dry" areas experience a decrease in freshwater. Geoengineering on the other hand experiences a rather large change in the freshwater flux patterns (except for the Pacific).

Looking more closely at Atlantic basin we see a strong increase in strength in the ITCZ for RCP and a decrease for geoengineering (see shift ITCZ below). The Northern Atlantic region (sinking region for AMOC) gets wetter in RCP while geoengineering gets drier in this region. The increase in freshwater flux (decrease) in RCP (geoengineering) is mainly caused by a decrease (increase) in evaporation over this region (see appendix fig. A1). Why the evaporation changes in this region for both fluxes and how this relates to the change in the AMOC lies beyond the scope of this paper.

The difference over time of SHF is in figures 5c and 5d. RCP has a strong increase in the Northern Atlantic and a slightly negative region over the Atlantic equator. Between Canada and Greenland there is small region with very strong outgoing flux, which corresponds to the location of the Gulf stream. This strong outgoing heat flux could be consequence of a weaker Gulf stream, which transport less heat to the north resulting in less heat being exchanged between the ocean and atmosphere. The sinking region in geoengineering has outgoing (negative) SHF losing heat to the atmosphere. Over the rest of the globe there are only two other regions with a noticeable difference over time. The anomalous downward (positive) flux over the East coasts of America and Japan could be explained by a weaker easterly jet.

To investigate the influence of the PE and SHF changes on the deep water formation we look at the changes in the buoyancy caused by both fluxes (to get the same units for both fluxes). Figures 5e and 5f show the buoyancy change for RCP due to the freshwater flux and surface heat flux respectively. Both figures show a similar pattern over the Atlantic but SHF has bigger positive impact on the buoyancy. This means decreased density in this region is mostly caused by the positive SHF here.

The buoyancy change in the geoengineering case (fig. 5f and 5h) stands out most in the Northern Atlantic, which is negative (increased density) for both fluxes. However again (same as RCP 8.5) the SHF has a larger

impact compared to PE. This means the buoyancy change in the most important sinking region of the AMOC is mostly defined by the surface heat flux.

ITCZ location

With the strong weakening of the AMOC in RCP there is less cross-equatorial ocean-heat transport northward, so we would expect a southward shift of the ITCZ, because there is less compensation necessary (also found in the literature for a weakened AMOC [32]). From figures 6a and especially 6c we can see that there is a very slight southward shift of the ITCZ (only ± 0.3 degrees). For geoengineering we expect to see a stable or very slight northward shift of the ITCZ due to the slight increase in strength for the AMOC (also found in the literature for a strengthened AMOC [33]). But we find a slightly larger shift compared to RCP southward movement of the ITCZ in the geoengineering case (0.35 degrees). Whether this shift is significant or not requires further investigation.

We chose the summer period because it shows a larger change in the ITCZ position compared to the winter. We excluded the spring and fall season because we wanted to see the shift in the position of the ITCZ at its maximal extend. The figures for the winter can be found in the appendix (A3a and A3b).

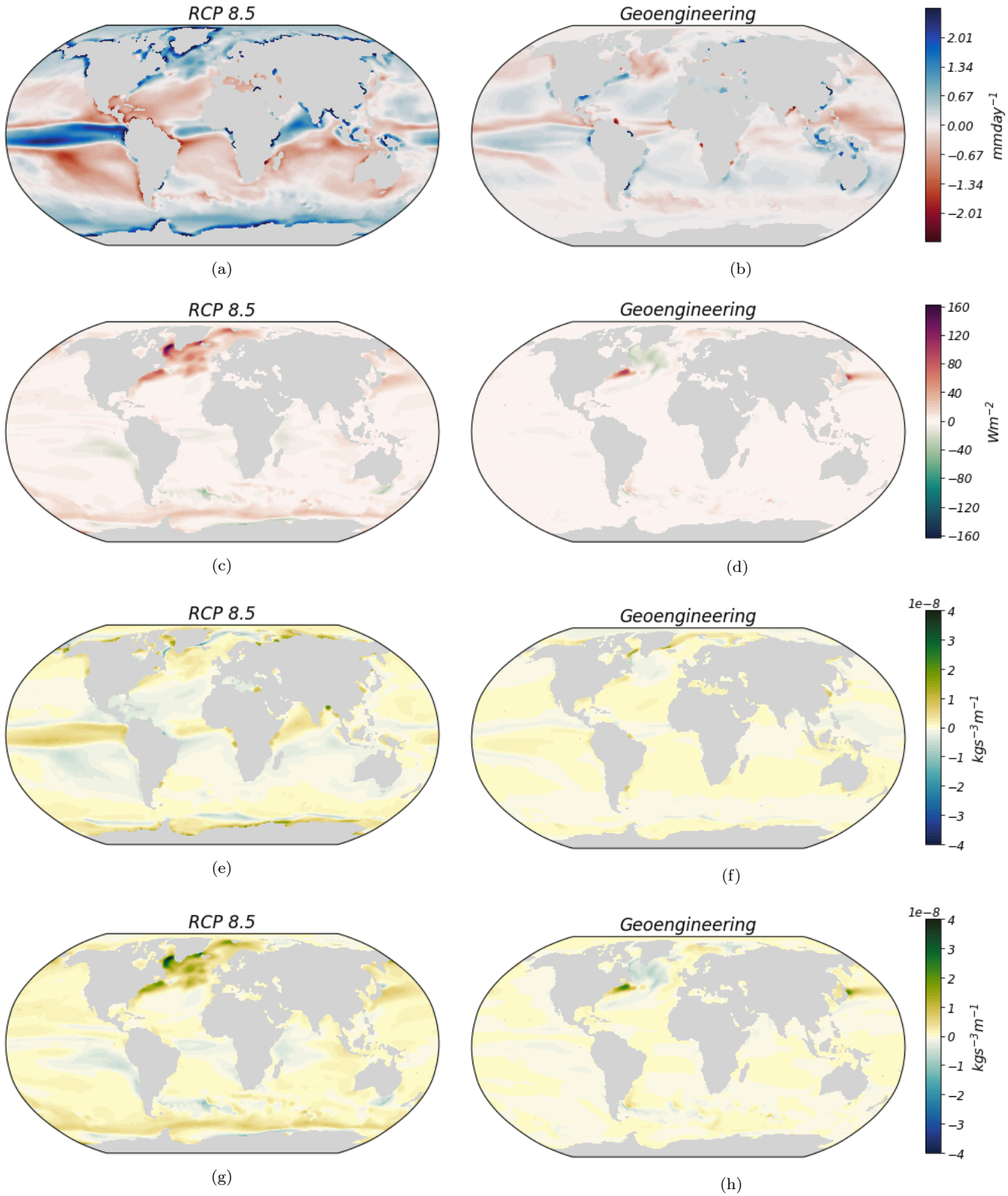

Figure 5: All figures show the difference between the first 25 years (2020-2045) and the last 25 years (2075-2100). The figures on the left side (5a, 5c, 5e, 5g) show the RCP 8.5 simulation and the right side (5b, 5d, 5f, 5h) show the geoengineering simulation. The positive values for the PE patterns in 5a and 5b indicate a increase in freshwater flux. The positive values for the SHF in 5c and 5d indicate a net downward radiation (warming of the surface). The positive values for 5e, 5f, 5g and 5h indicate an increase in the buoyancy. 5e and 5f are the buoyancy flux derived from the change in the freshwater content. 5g and 5g are the buoyancy flux derived from the change in SHF

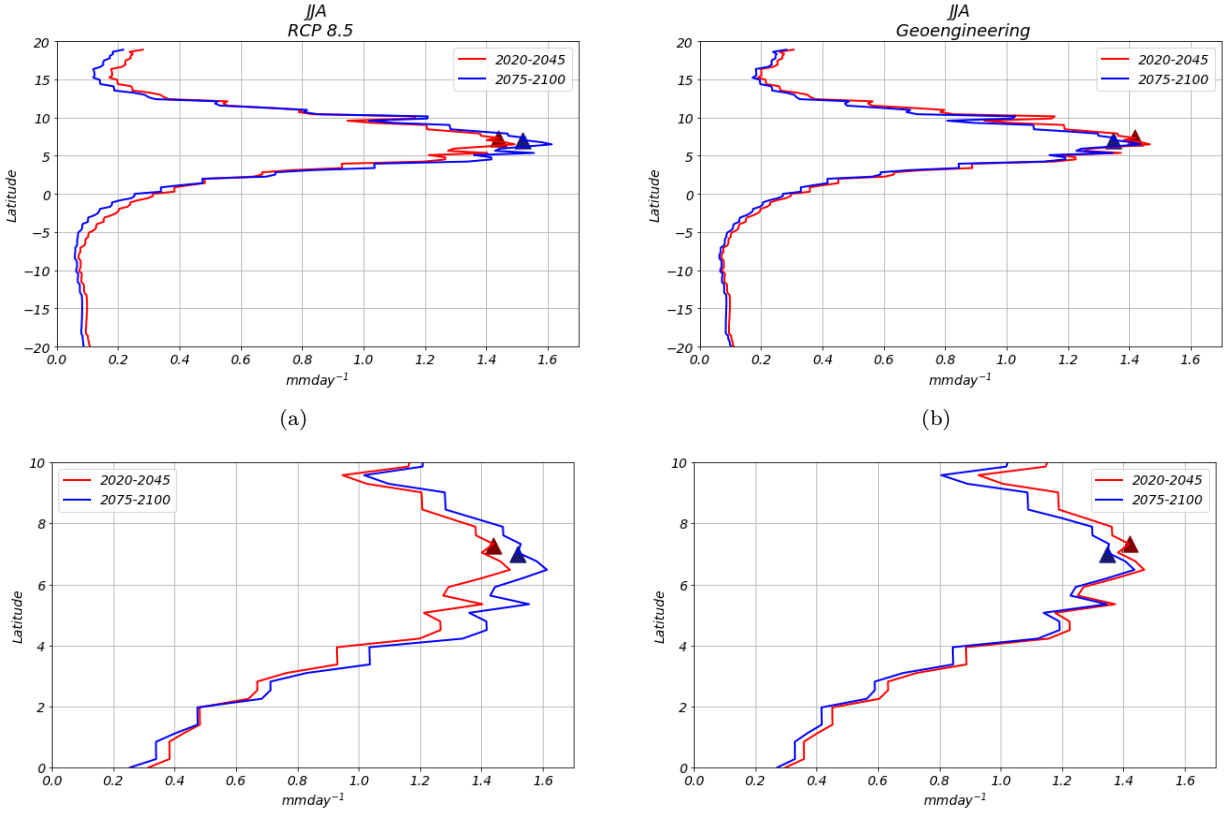

(a) (b) (c) (d)

Figure 6: July, June and August yearly averages. The solid lines indicate area weighted values of precipitation and the triangles indicate weighted values following equation (1). 6c and 6d are zoomed in between the equator and 10 degrees north.

3.2 Salinity budget

We computed the Mov stability criterion for both the southern and northern boundary of the Atlantic basin (see fig. 7a). Positive values for the southern and negative values for the northern boundary indicate a monostable regime with convergence of freshwater into the Atlantic basin. Both RCP and geoengineering show the same monostable regime, with a notable difference in that RCP has a clear downward trend from 2040 till the end of the simulation. This downward trend is also visible in the ΣMov in figure 7b, which indicates a less stable AMOC in RCP compared to geoengineering.

To check the veracity of these results we computed the complete freshwater budget from equation (2) without the subscale transport term, R (fig. 7d). From this we can see that the freshwater influx from evaporation, precipitation and melt (EPR) follow the same trend as the transport terms Mov, Maz and the change of the freshwater content Q_t. From the sum of the Mov and Maz (both north and south components, see fig. A2) we find that these are almost in complete balance meaning that the trends found in the freshwater flux must be caused by a change in the freshwater content of the Atlantic basin.

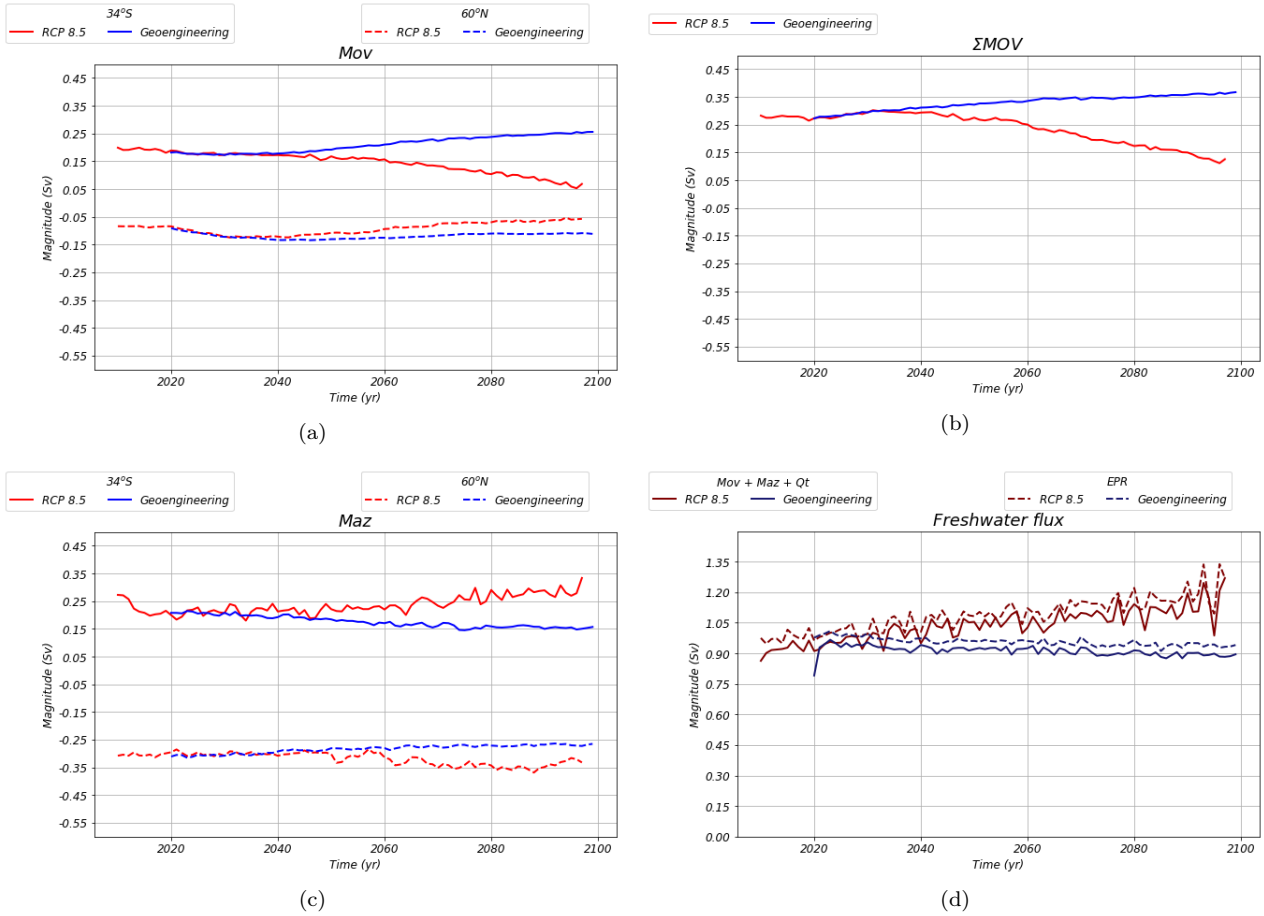

Figure 7: For all figures the red lines indicate the RCP simulation and the blue lines the geoengineering. The solid lines in 7a (7c) are the Mov (Maz) at 34S and the dotted lines are the Mov (Maz) at 60N. The freshwater flux (7d) is the comparison between EPR (dashed line) and the sum of the Mov, Maz (both north and south) and Q_t.

4 Conclusion

In this paper we looked at the change in the AMOC strength under two simulations, one with only RCP 8.5 forcing and one with added geoengineering to limit global warming to 2020 levels. We found that the AMOC strength increases with the use of geoengineering compared to strong weakening under RCP. This difference in strength is likely caused by the changing patterns in the surface fluxes of heat and freshwater. In the pattern of these fluxes we found that both fluxes decrease the buoyancy in the Labrador and Greenland sea under geoengineering compared to an increase under RCP 8.5 only. Important to note here is that only sea-ice is modelled here. The changes in the land-ice could have a large impact on the freshwater balance in the Northern Atlantic.

An expected result of this increase in strength would be the northward shift of the ITCZ to balance the change in the cross-equatorial heat transport. We found in a simple test for the seasonal mean ITCZ position over the Atlantic that this does not happen. This unexpected result is likely caused by keeping the interhemisphere temperature (T1) gradient constant [34].

There has been much research into the continued weaking of the AMOC over the twenty-first century and if this weakening could lead to a complete collapse in the future. In this research we found that the AMOC under the injection of sulphate aerosols is not only much stronger compared to a RCP 8.5 scenario, but is also more stable. The Mov criterion did not show a bistable regime for the RCP 8.5, but had a strong downward trend till the end of the simulation, so we might be approaching bistability.

The injection strategy chosen in the geoengineering project has a positive effect on the AMOC, but a lot more studies are required to learn more about different injection strategies. Before implementation of geoengineering is even considered there is also need to be additional studies in all the other possible side-effects of injection sulphate aerosols in the stratosphere. The use of SRM should always be viewed as a sort of last resort and not as a substitute for large-scale mitigation.

To increase our understanding of the AMOC a further study using a non-transient CO_2 forcing (4xCO_2) could be used to get a clearer view of the impact of geoengineering on a equilibrated climate.

References

[1] J. Rogelj, M. den Elzen, N. Höhne, T. Fransen, H. Fekete, H. Winkler, R. Schaeffer, F. Sha, K. Riahi, and M. Meinshausen, "Paris Agreement climate proposals need a boost to keep warming well below 2 °C," 2016.

[2] Z. Zhang, J. C. Moore, D. Huisingh, and Y. Zhao, "Review of geoengineering approaches to mitigating climate change," *Journal of Cleaner Production*, vol. 103, pp. 898–907, 2015.

[3] D. P. Keller, E. Y. Feng, and A. Oschlies, "Potential climate engineering effectiveness and side effects during a high carbon dioxide-emission scenario," *Nature Communications*, vol. 5, pp. 1–11, 2014.

[4] D. G. MacMartin and B. Kravitz, "Mission-driven research for stratospheric aerosol geoengineering," *Proceedings of the National Academy of Sciences*, 2019.

[5] J. McClellan, D. W. Keith, and J. Apt, "Cost analysis of stratospheric albedo modification delivery systems," *Environmental Research Letters*, vol. 7, no. 3, 2012.

[6] A. Robock, "20 Reasons Why Geoengineering May Be a Bad Idea," *Bulletin of the Atomic Scientists*, vol. 64, no. 2, pp. 14–18, 2008.

[7] K. Kuhlbrodt, A. Griesel, M. Montoya, A. Levermann, M. Hofmann, and S. Rahmstorf, "On the driving processes of the Atlantic meridional overturning circulation," *Reviews of Geophysics*, vol. 45, no. 2, pp. 20584–20589, 2007.

[8] L. Caesar, S. Rahmstorf, A. Robinson, and G. Feulner, "Article Observed fingerprint of a weakening Atlantic Ocean overturning circulation," 2018.

[9] P. Bakker, A. Schmittner, J. T. Lenaerts, A. Abe-Ouchi, D. Bi, M. R. van den Broeke, W. L. Chan, A. Hu, R. L. Beadling, S. J. Marsland, S. H. Mernild, O. A. Saenko, D. Swingedouw, A. Sullivan, and J. Yin, "Fate of the Atlantic Meridional Overturning Circulation: Strong decline under continued warming and Greenland melting," *Geophysical Research Letters*, vol. 43, no. 23, pp. 12,252–12,260, 2016.

[10] H. Stommel and P. Hall, "Thermohahe Convection with Two Stable Regimes of flow," *Tellus*, vol. 11, pp. 224–230, 1961.

[11] S. Drijfhout, E. Gleeson, H. A. Dijkstra, and V. Livina, "Spontaneous abrupt climate change due to an atmospheric blocking-sea-ice-ocean feedback in an unforced climate model simulation," *Proceedings of the National Academy of Sciences*, 2013.

[12] S. Rahmstorf, "Ocean circulation and climate during the past 120,000 years," *Nature*, vol. 419, no. 6903, pp. 207–214, 2002.

[13] J. T. Fasullo, S. Tilmes, J. H. Richter, B. Kravitz, D. G. MacMartin, M. J. Mills, and I. R. Simpson, "Persistent polar ocean warming in a strategically geoengineered climate," *Nature Geoscience*, vol. 11, no. 12, pp. 910–914, 2018.

[14] H. A. Dijkstra, *Dynamical oceanography.* 2008.

[15] D. F. Uk, G. F. Uk, N. Zealand, and M. K. France, "Information from paleoclimate archives," *Climate Change 2013 the Physical Science Basis: Working Group I Contribution to the Fifth Assessment Report of the Intergovernmental Panel on Climate Change*, 2013.

[16] J. Marshall, A. Donohoe, D. Ferreira, and D. McGee, "The ocean's role in setting the mean position of the Inter-Tropical Convergence Zone," *Climate Dynamics*, vol. 42, no. 7-8, pp. 1967–1979, 2014.

[17] S. Tilmes, J. H. Richter, B. Kravitz, D. G. MacMartin, M. J. Mills, I. R. Simpson, A. S. Glanville, J. T. Fasullo, A. S. Phillips, J.-F. Lamarque, J. Tribbia, J. Edwards, S. Mickelson, and S. Gosh, "CESM1(WACCM) Stratospheric Aerosol Geoengineering Large Ensemble (GLENS) Project," *Bulletin of the American Meteorological Society*, vol. 1, pp. BAMS–D–17–0267.1, 2018.

[18] J. W. Hurrell, M. Holland, P. R. Gent, S. Ghan, J. E. Kay, P. J. Kushner, J.-F. Lamarque, W. Large, D. Lawrence, K. Lindsay, W. H. Lipscomb, M. C. Long, N. Mahowald, D. R. Marsh, R. B. Neale, P. Rasch, S. Vavrus, M. Vertenstein, D. Bader, W. Collins, J. Hack, J. Kiehl, and S. Marshall, "The Community Earth System Model: A Framework for Collaborative Research," *Bulletin of the American Meteorological Society*, no. SEPTEMBER, p. 130204122247009, 2013.

[19] X. Liu, R. C. Easter, S. J. Ghan, R. Zaveri, P. Rasch, X. Shi, J. F. Lamarque, A. Gettelman, H. Morrison, F. Vitt, A. Conley, S. Park, R. Neale, C. Hannay, A. M. Ekman, P. Hess, N. Mahowald, W. Collins, M. J. Iacono, C. S. Bretherton, M. G. Flanner, and D. Mitchell, "Toward a minimal representation of aerosols in climate models: Description and evaluation in the Community Atmosphere Model CAM5," *Geoscientific Model Development*, vol. 5, no. 3, pp. 709–739, 2012.

[20] D. P. van Vuuren, J. Edmonds, M. Kainuma, K. Riahi, A. Thomson, K. Hibbard, G. C. Hurtt, T. Kram, V. Krey, J. F. Lamarque, T. Masui, M. Meinshausen, N. Nakicenovic, S. J. Smith, and S. K. Rose, "The representative concentration pathways: An overview," *Climatic Change*, vol. 109, no. 1, pp. 5–31, 2011.

[21] B. Kravitz, D. G. MacMartin, M. J. Mills, J. H. Richter, S. Tilmes, J.-F. Lamarque, J. J. Tribbia, and F. Vitt, "First simulations of designing stratospheric sulfate aerosol geoengineering to meet multiple simultaneous climate objectives," *Journal of Geophysical Research: Atmospheres*, 2017.

[22] K. C. Bala Govindasamy, "Geoengineering Earth's radiation balance to mitigate CO2-induced climate change," vol. 27, no. 14, pp. 1–4, 2007.

[23] D. G. MacMartin and B. Kravitz, "The Engineering of Climate Engineering," *Annual Review of Control, Robotics, and Autonomous Systems*, pp. 1–24, 2018.

[24] A. E. Gill, *Atmosphere-Ocean Dynamics*. 30 ed., 1982.

[25] O. Adam, T. Bischoff, and T. Schneider, "Seasonal and interannual variations of the energy flux equator and ITCZ. Part I: Zonally averaged ITCZ position," *Journal of Climate*, vol. 29, no. 9, pp. 3219–3230, 2016.

[26] H. A. Dijkstra, "Characterization of the multiple equilibria regime in a global ocean model," *Tellus, Series A: Dynamic Meteorology and Oceanography*, vol. 59, no. 5, pp. 695–705, 2007.

[27] M. den Toom, H. A. Dijkstra, W. Weijer, M. W. Hecht, M. E. Maltrud, and E. van Sebille, "Response of a Strongly Eddying Global Ocean to North Atlantic Freshwater Perturbations," *Journal of Physical Oceanography*, vol. 44, no. 2, pp. 464–481, 2013.

[28] S. Rahmstorf, "On the freshwater forcing and transport of the Atlantic thermohaline circulation," pp. 799–811, 1996.

[29] P. R. Gent, "A commentary on the Atlantic meridional overturning circulation stability in climate models," *Ocean Modelling*, vol. 122, no. June 2017, pp. 57–66, 2018.

[30] W. Liu and Z. Liu, "A diagnostic indicator of the stability of the atlantic meridional overturning circulation in CCSM3," *Journal of Climate*, vol. 26, no. 6, pp. 1926–1938, 2013.

[31] G. McCarthy, E. Frajka-Williams, W. E. Johns, M. O. Baringer, C. S. Meinen, H. L. Bryden, D. Rayner, A. Duchez, C. Roberts, and S. A. Cunningham, "Observed interannual variability of the Atlantic meridional overturning circulation at 26.5°N," *Geophysical Research Letters*, vol. 39, no. 19, pp. 1–5, 2012.

[32] R. Zhang and T. L. Delworth, "Simulated tropical response to a substantial weakening of the Atlantic thermohaline circulation," *Journal of Climate*, vol. 18, no. 12, pp. 1853–1860, 2005.

[33] M. Vellinga and P. Wu, "Low-latitude freshwater influence on centennial variability of the Atlantic thermohaline circulation," *Journal of Climate*, vol. 17, no. 23, pp. 4498–4511, 2004.

[34] B. Kravitz, D. G. Macmartin, H. Wang, and P. J. Rasch, "Geoengineering as a design problem," *Earth System Dynamics*, vol. 7, no. 2, pp. 469–497, 2016.

A Figures

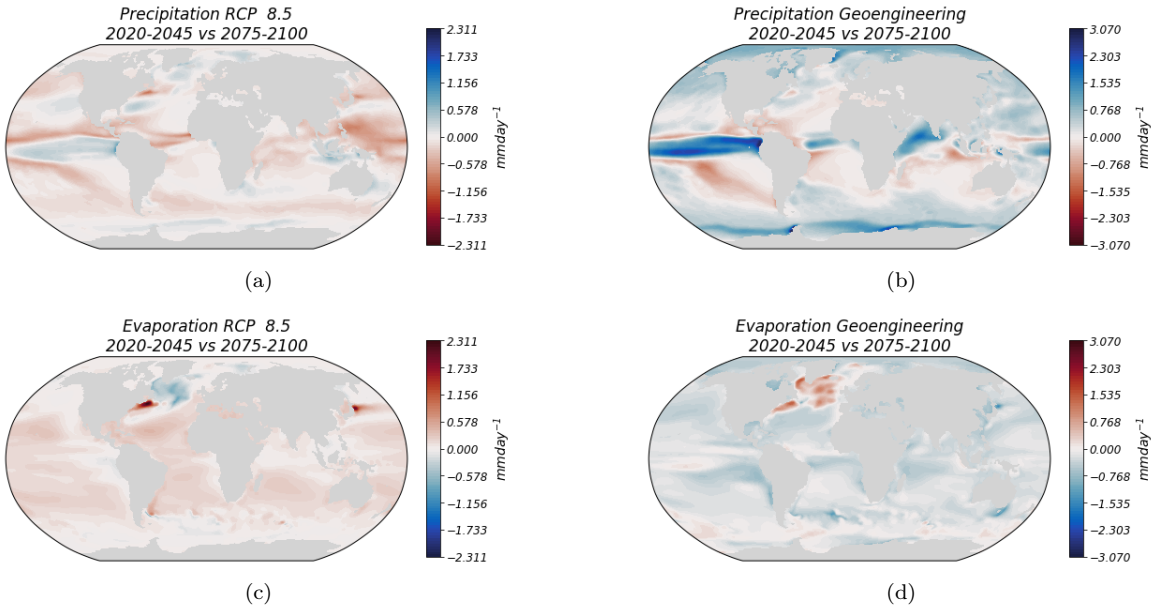

Figure A1: All figures show the difference between the first 25 years (2020-2045) and the last 25 years (2075-2100). The figures on the left side (A1a, **??** show RCP and the right side (A1b, A1d show geoengineering. Positive values indicate an increase (decrease) in freshwater for A1a (**??**) and A1b(A1d)

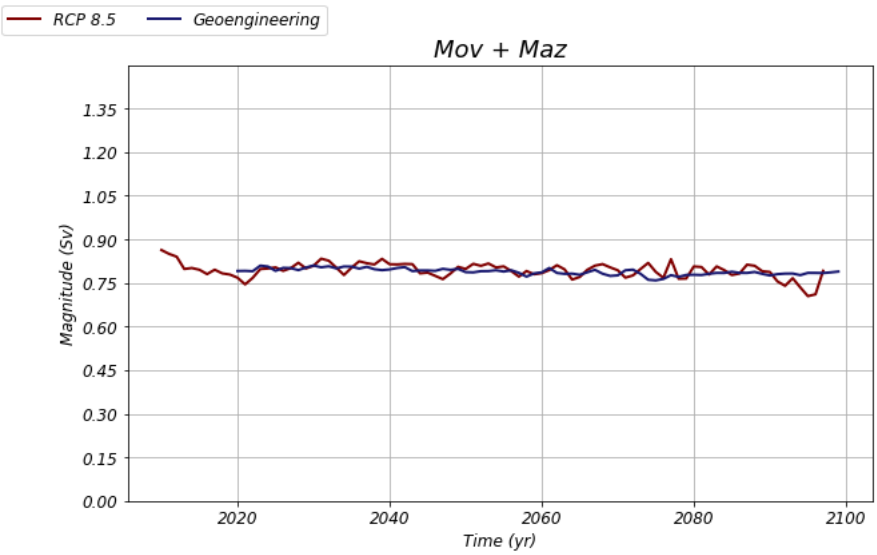

Figure A2: Sum of the north and south components of the Mov and Maz

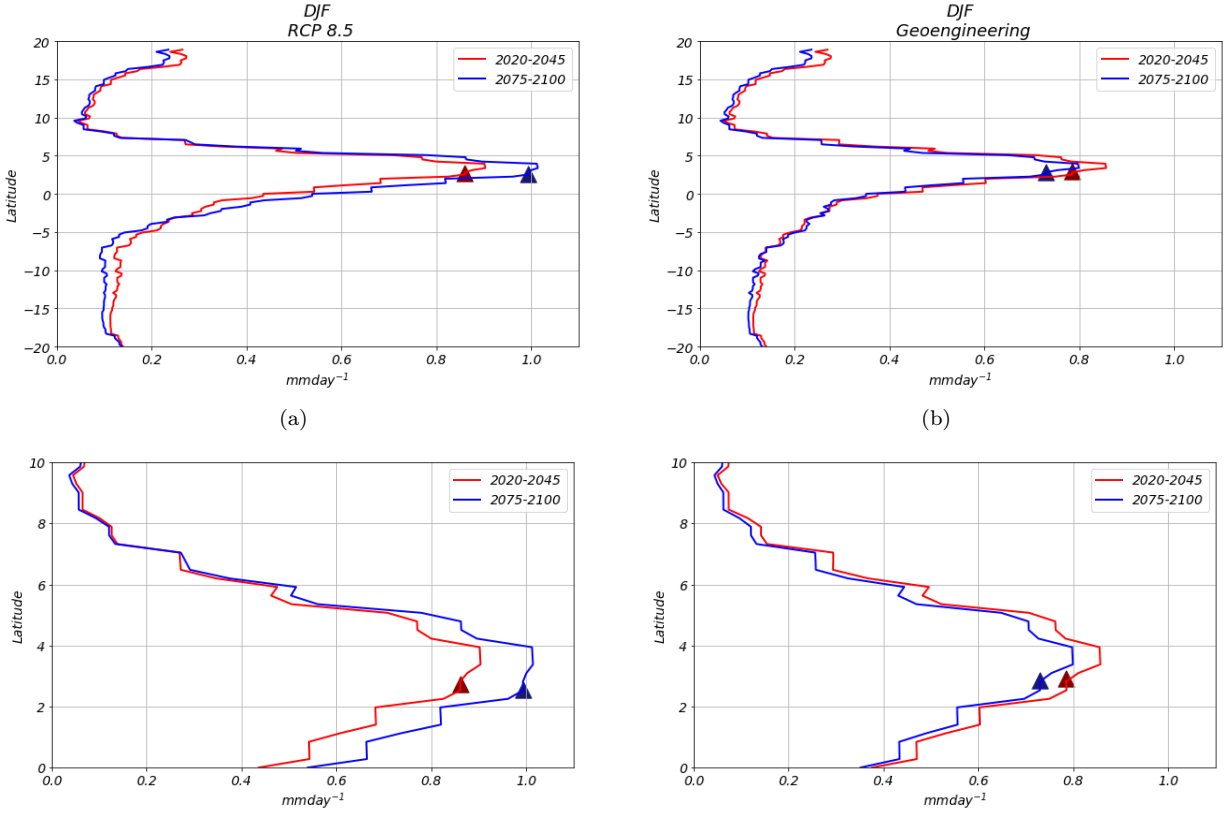

Figure A3: December, January, February yearly averages. The solid lines indicate area weighted values of precipitation and the triangles indicate weighted values following equation (1). A3c and A3d are zoomed in between the equator and 10 degrees north.